Supplement of Atmos. Meas. Tech., 15, 4503–4529, 2022
https://doi.org/10.5194/amt-15-4503-2022-supplement

Atmospheric Measurement Techniques
Open Access

Supplement of

Horizontal distribution of tropospheric NO_2 and aerosols derived by dual-scan multi-wavelength multi-axis differential optical absorption spectroscopy (MAX-DOAS) measurements in Uccle, Belgium

Ermioni Dimitropoulou et al.

Correspondence to: Ermioni Dimitropoulou (ermioni.dimitropoulou@aeronomie.be)

Table S1. DOAS settings for O_4 and NO_2 in the six different fitting intervals.

Fitting window/ nm	Reference wavelength/ nm	Molecule	Reference
330 – 361	343	BrO (223 K)	Fleischmann et al. (2004)
350 - 370	360	O_4	Finkenzeller, H. (private communication)
		NO_2 (298 K)	Vandaele et al. (1998) with I_o correction (SCD of 10^{17} molec.cm^{-2})
		O_3 (223 K)	Serdyuchenko et al. (2014) with I_0 correction (SCD of 10^{20} molecules/cm^2)
		HCHO (297 K)	Meller and Moortgat (2000)
		O_3 (243 K)	Pre-orthogonalized Serdyuchenko et al. (2014) with I_0 correction (SCD of 10^{20} molecules/cm^2)
		Ring	Pseudo cross-section according to Chance and Spurr (1997) and normalized as in Wagner et al. (2009)
		Polynomial	Order 3 (4 coefficients)
360-383.5	380	BrO	Fleischmann et al. (2004)
		O_4	Finkenzeller, H. (private communication)
		NO_2 (298 K)	Vandaele et al. (1998) with I_o correction (SCD of 10^{17} molec.cm^{-2})
		NO_2 (220 K)	Pre-orthogonalized Vandaele et al. (1998) with I_0 correction
		Ring	Pseudo cross-section according to Chance and Spurr (1997) and normalized as in Wagner et al. (2009)
		Polynomial	Order 5 (6 coefficients)
420-460	447	NO_2 (298 K)	Vandaele et al. (1998) with I_o correction (SCD of 10^{17} molec.cm^{-2})
450 - 490	477		
		O_4 (293 K)	Thalman and Volkamer (2013)

		O_3 (223 K)	Serdyuchenko et al. (2014) with I_0 correction (SCD of 10^{20} molecules/cm^2)
		H_2O	HITRAN (Rothman et al., 2013)
		NO_2 (220 K)	Pre-orthogonalized Vandaele et al. (1998) with I_0 correction
		Ring	Pseudo cross-section according to Chance and Spurr (1997) and normalized as in Wagner et al. (2009)
		Polynomial	Order 3 (4 coefficients)
510 – 540.1	530	NO_2 (298 K)	Vandaele et al. (1998) with I_o correction (SCD of 10^{17} molec.cm^{-2})
		O_4 (293 K)	Thalman and Volkamer (2013)
		O_3 (223 K)	Serdyuchenko et al. (2014) with I_0 correction (SCD of 10^{20} molecules/cm^2)
		H_2O	HITRAN (Rothman et al., 2013)
		NO_2 (220 K)	Pre-orthogonalized Vandaele et al. (1998) with I_0 correction
		Ring	Pseudo cross-section according to Chance and Spurr (1997) and normalized as in Wagner et al. (2009)
		Polynomial	Order 2 (3 coefficients)

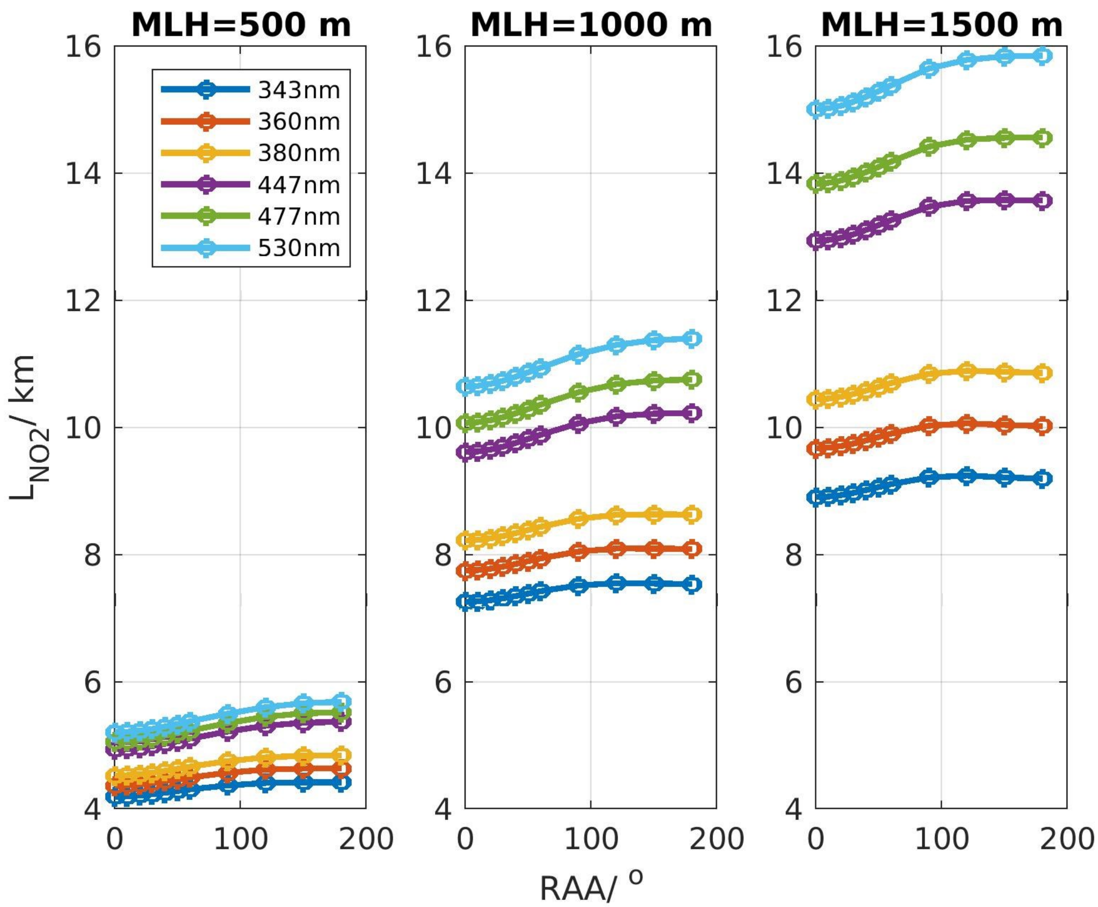

Figure S1. Simulated L_{NO2} as a function of the RAA for different MLH_{NO2} values (from left to right panel: MLH_{NO2} equal to 500 m, 1000 m, and 1500 m), wavelengths, one SZA value (30°), and one AOD value (0.3).

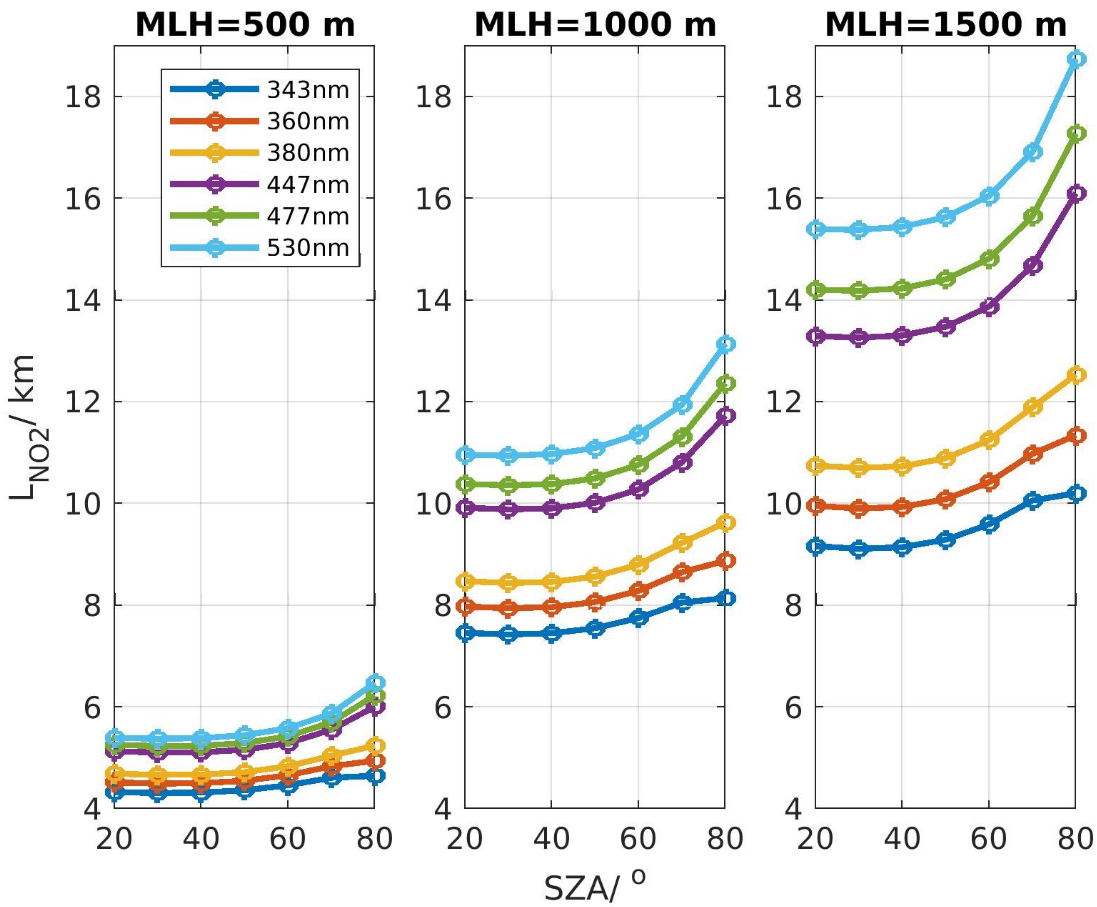

Figure S2. Simulated L_{NO2} as a function of the SZA for different MLH_{NO2} values (from left to right panel: MLH_{NO2} equal to 500 m, 1000 m, and 1500 m), wavelengths, one RAA value (60°), and one AOD value (0.3).

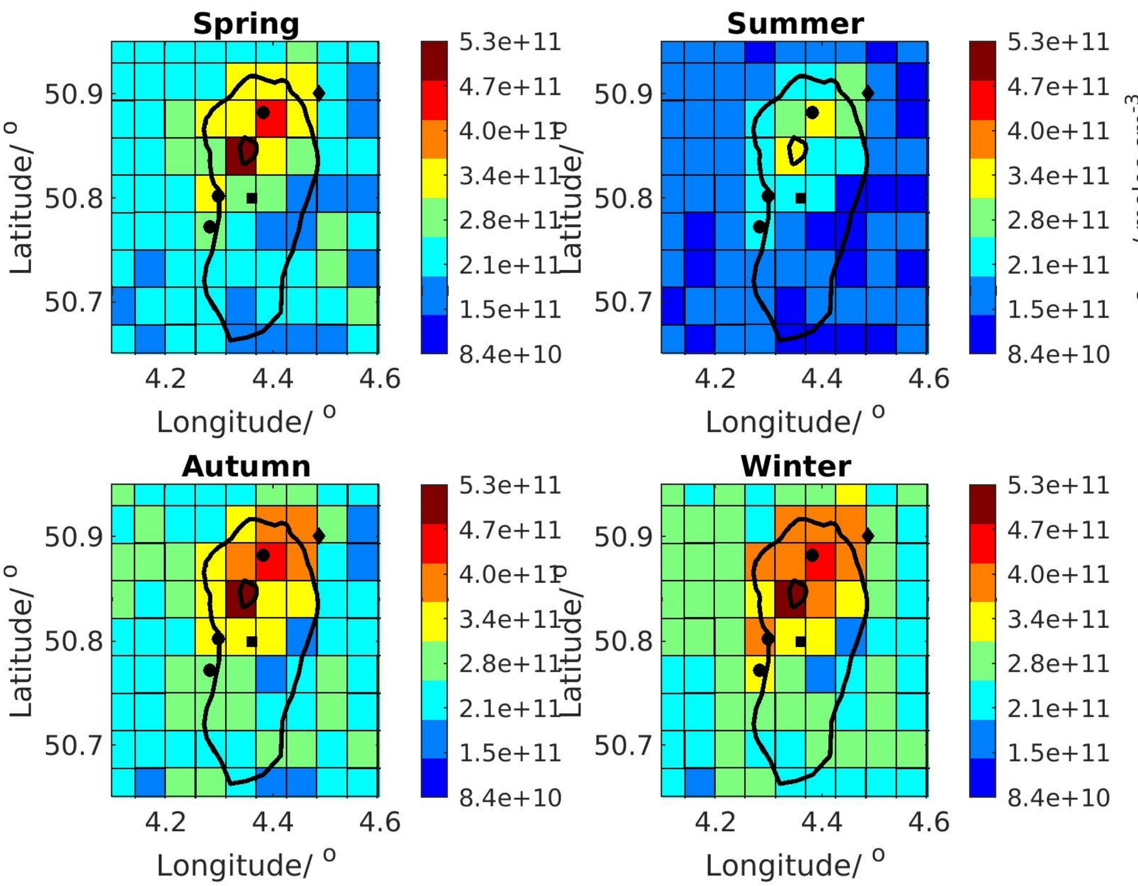

Figure S3. Seasonal near-surface NO_2 concentration grids as estimated over Brussels by the RIO air-quality model. The black square shows the MAX-DOAS position, the black polygon the National Airport, the black dots the NO_2 hotspots, and the black line represents the Brussels Ring motorway.

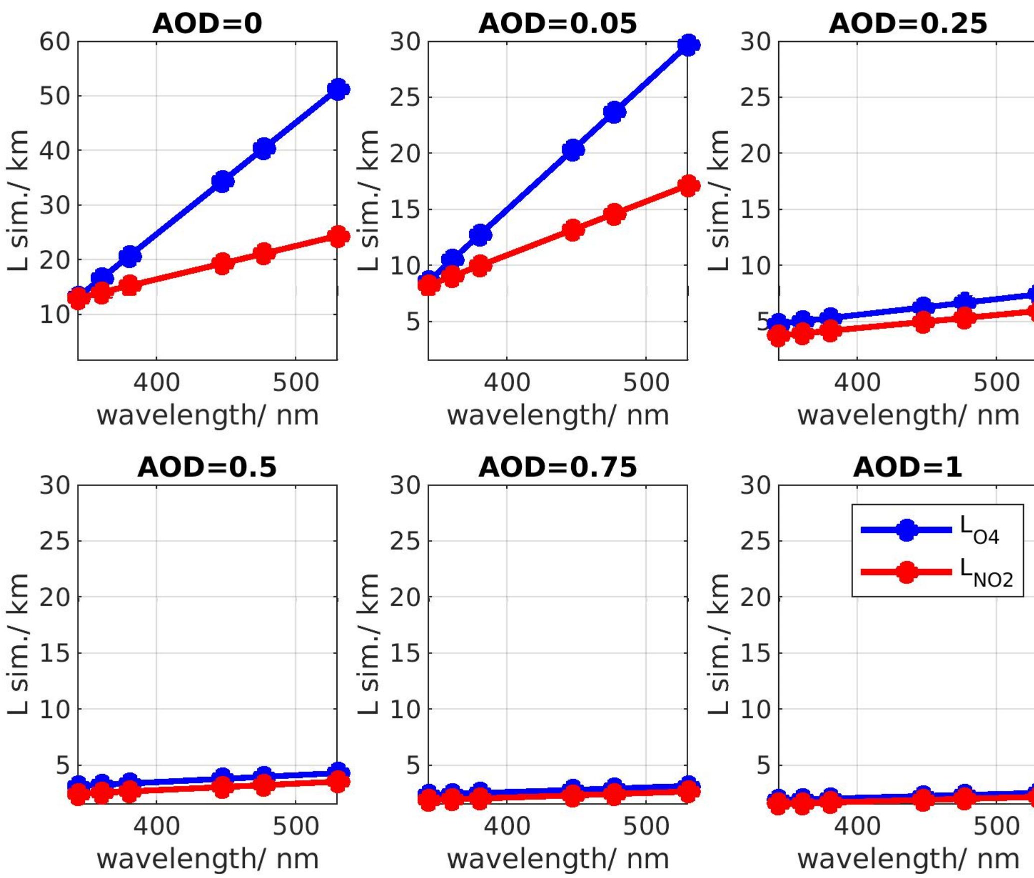

Figure S4. Simulated differential effective light path of O_4 dSCDs (L_{O4} sim.) and NO_2 dSCDs (L_{NO2} sim.) as a function of wavelength for different AOD scenarios.

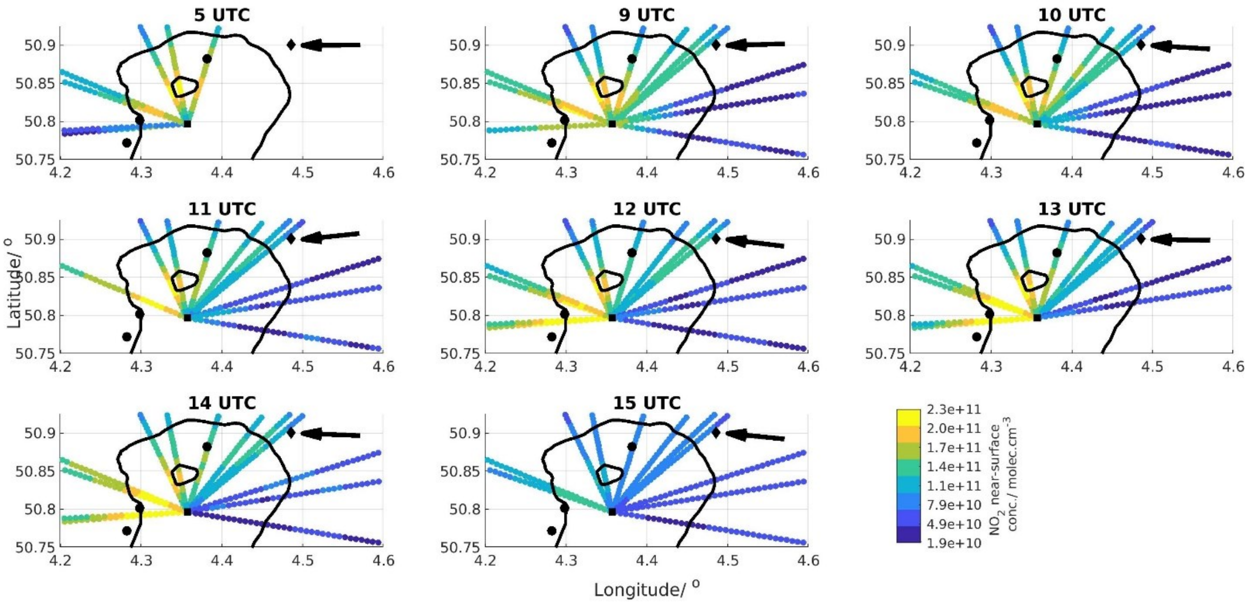

Figure S5. Maps of hourly averaged NO_2 near-surface concentration horizontal profiles per azimuthal direction for June 28, 2019. The wind direction is shown with the black arrow. The black square shows the MAX-DOAS instrument location, the black polygon the National Airport, the black dots the NO_2 hotspots emitting more than 10 kg of NO_x per hour (Emission Inventory of the Belgian Interregional Environment Agency, 2017) , and the black line represents the Brussels Ring road.

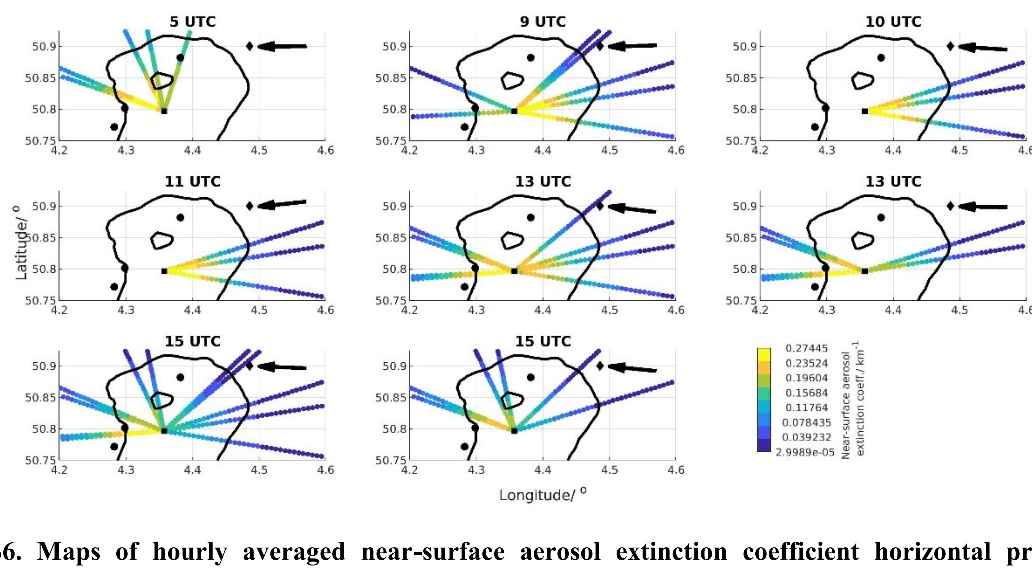

Figure S6. Maps of hourly averaged near-surface aerosol extinction coefficient horizontal profiles per azimuthal direction for June 28, 2019. The wind direction is shown with the black arrow. The black square

shows the MAX-DOAS instrument location, the black polygon the National Airport, the black dots the NO_2 hotspots emitting more than 10 kg of NO_x per hour (Emission Inventory of the Belgian Interregional Environment Agency, 2017) , and the black line represents the Brussels Ring road.

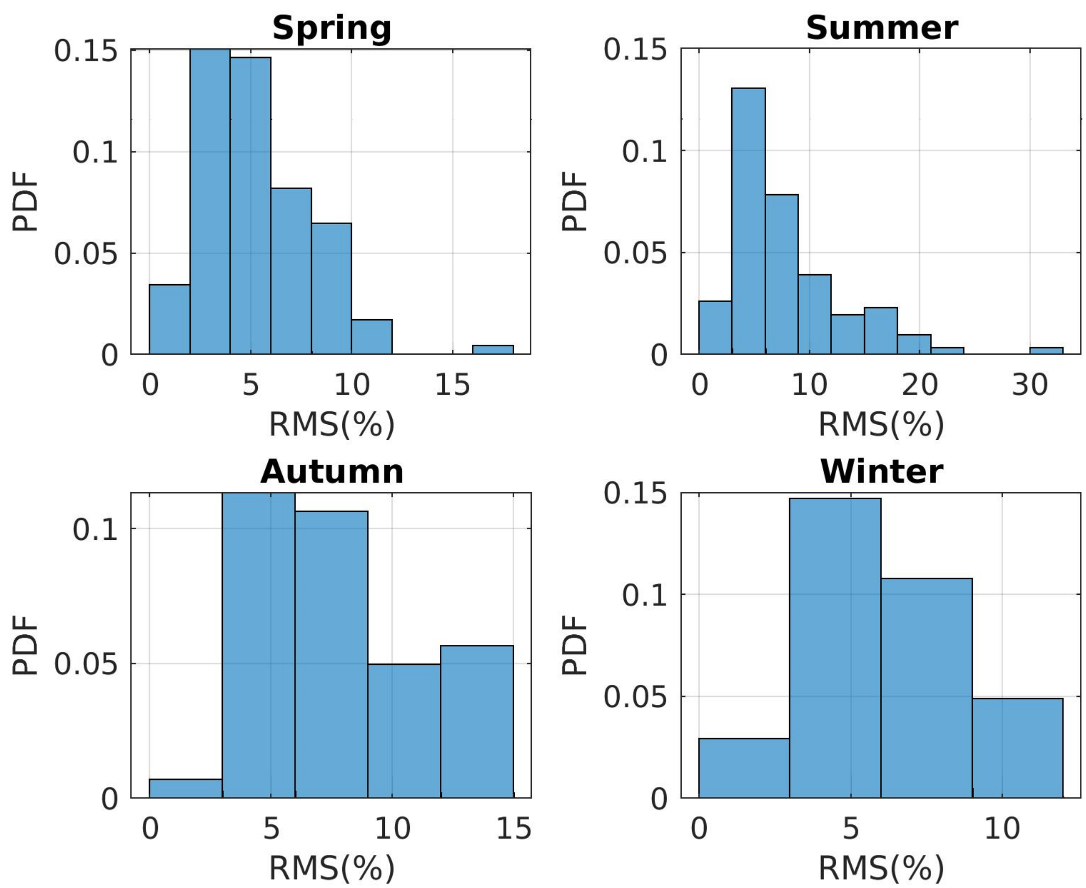

Figure S7. Seasonal histograms of the Probability Density Function (PDF) of the calculated RMS (%) between measured and retrieved NO_2 near-surface concentrations of the horizontal retrieval (see Table 3).

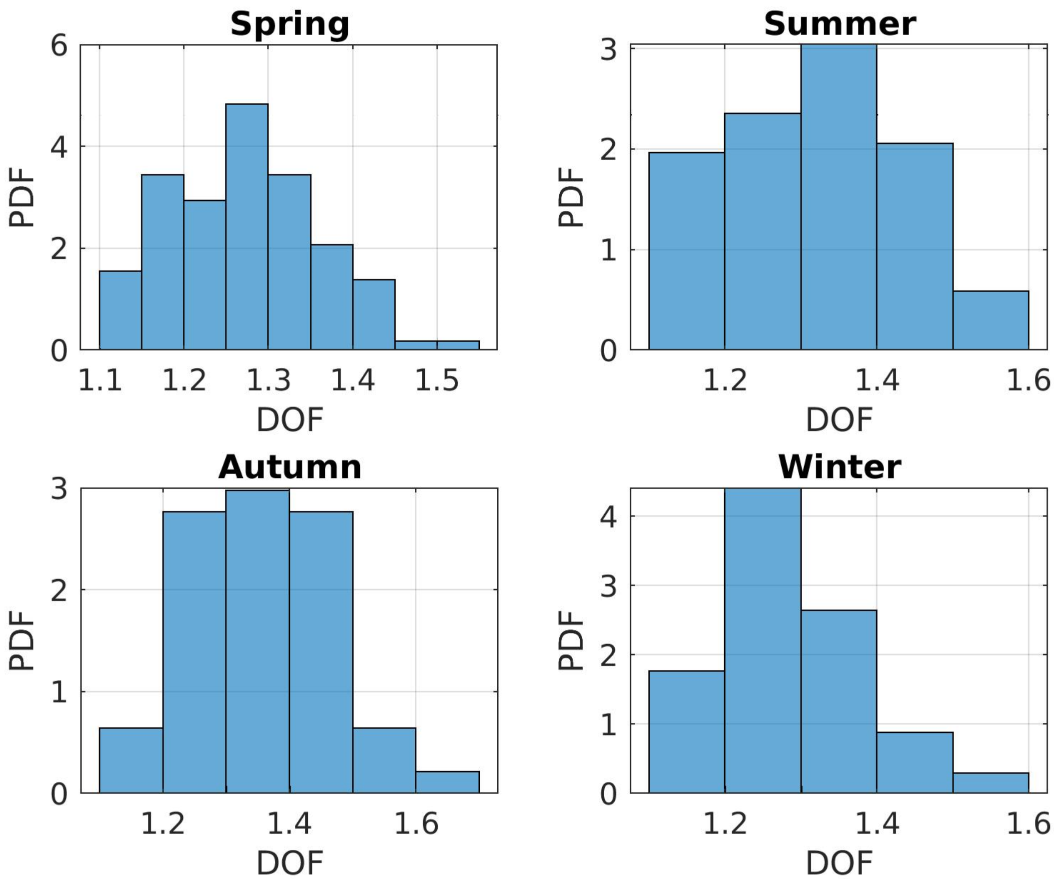

Figure S8. Seasonal histograms of the Probability Density Function (PDF) of the degrees of freedon (DOFS) of the horizontal retrieval (see Table 3).

S1 MAX-DOAS horizontal NO_2 distribution versus air quality model data

The RIO air quality model over the Brussels-Capital Region is used to validate the retrieved near-surface NO_2 concentration horizontal profiles.

RIO is a land-use regression model based on the interpolation of the hourly NO_2 near-surface concentrations measured by the in-situ telemetric air quality network in Brussels (Hooyberghs et al., 2006; Janssen et al., 2008). RIO model provides hourly NO_2 concentration maps on a 4x4 km^2 spatial resolution.

To compare the RIO and MAX-DOAS near-surface NO_2 concentrations, the following steps have been followed:

1. One year (March 2018 – December 2018) of RIO and MAX-DOAS observations have been used.
2. The MAX-DOAS near-surface NO2 concentrations are hourly averaged in each azimuthal direction.
3. The MAX-DOAS near-surface NO2 concentrations on the horizontal segment crossing a RIO pixel (i.e., 4x4 km^2) and located inside each pixel are averaged,
4. Pixel-to-pixel comparison between the two datasets has been performed.

Figure S9 shows the seasonal correlation plots for March 2018 – December 2018. The higher correlation coefficients are found during spring (R=0.82) and autumn (R=0.75), while lower correlations are reported in summer (R=0.64) and winter (R=0.51).

During all seasons, the slope values are quite small (s in the range of 0.25-0.50). Given the fact that the RIO model is based in in-situ observations, this finding is excepted. The interested reader is referred to Dimitropoulou et al. (2020).

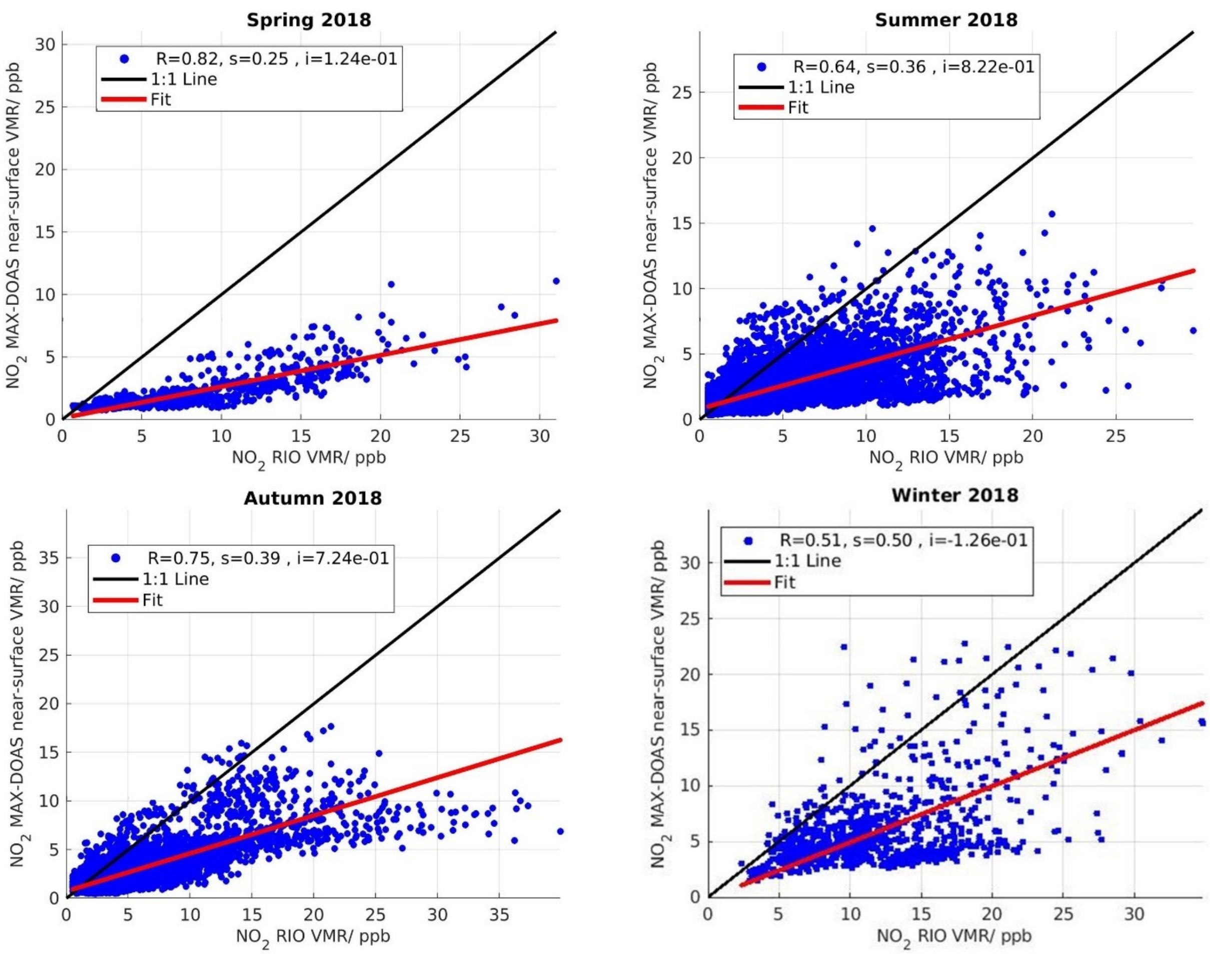

Figure S9. Seasonal scatter plots of near-surface NO_2 VMRs derived from the dual-scan MAX-DOAS and RIO observations over the Brussels-Capital Region.

S2 Investigation of the a priori NO_2 profile shape and clouds in TROPOMI NO_2 retrievals

Three additional comparisons were conducted in this study. First, a TROPOMI tropospheric NO_2 column product (DDSv2 product) with an improved FRESCO-S cloud retrieval was tested. As discussed in Dimitropoulou et al. (2020), clouds can significantly affect tropospheric NO_2 VCD retrievals from satellite observations. The dataset is available for four different periods in 2018 – 2019 (see Sect. 3). Fig. S10a and S10b show that the slope value increases by about 29% (equal to 0.49 instead of 0.38 for the baseline product), as well as the correlation coefficient between both datasets (R equal to 0.73 instead of 0.467. This is in agreement with the TROPOMI Routine Operations Consolidated Validation Report (ROCVR; https://mpc-vdaf.tropomi.eu/), where the use of the improved FRESCO-wide resulted in a bias reduction with respect to ground-based NO_2 data.

Secondly, a new TROPOMI data product covering the November 2018 to February 2020 period is used. In this product, the coarse TM5-MP a priori NO_2 profiles are replaced by NO_2 profile shapes from the CAMS regional CTM ensemble at a spatial resolution of 0.1° x 0.1° (S5P-CAMS product; Douros et al., in preparation; Ialongo et al., 2019; Tack et al., 2021). As can be seen in Fig. S10c and S10d, using a spatially finer a priori NO_2 vertical profile improves slightly the slope value, which is equal to 0.68 (instead of 0.60 for the baseline TROPOMI product). This represents an increase of the slope by about 13%. This finding indicates that part of the TROPOMI underestimation of tropospheric NO_2 columns is caused by inadequate a priori profiles in the TROPOMI retrievals for urban conditions. On the other hand, the fact that the slope value is still lower than unity, even when CAMS regional a priori profiles are used, indicate that other factors contribute to the TROPOMI underestimation or that CAMS profiles are still sub-optimal, as suggested by results obtained when applying MAX-DOAS profiles to TROPOMI (see below).

Finally, the impact of the a priori profile in the TROPOMI NO_2 retrieval is investigated using MAX-DOAS profile data. For this test, TROPOMI NO_2 columns are recalculated, similarly as in Dimitropoulou et al. (2020), using daily median MAX-DOAS vertical profiles derived in the main azimuthal direction by applying the MMF inversion algorithm. Those TROPOMI NO_2 columns are then compared to the horizontally-resolved MAX-DOAS data, as in Sect. 6.4. Figure S11 presents the comparison results per season. When comparing it with Fig. 23, we find that the change in the NO_2 vertical profile shape improves the slope value in the comparison with ground-based observations. Except for winter, the slopes are improved (slopes in the 0.68 - 1.02 range) due to an increase of the recalculated TROPOMI columns. This result confirms once again that the a priori profile in the TROPOMI retrieval is a key player in the TROPOMI underestimation of tropospheric NO_2 columns in urban conditions, as already stated in previous studies (see e.g. Dimitropoulou et al., 2020; Ialongo et al., 2019; Tack et al., 2021). The present study suggests that in urban conditions, the NO_2 profile shapes from the CAMS regional CTM ensemble are not the most suitable a priori information that can be applied in the TROPOMI retrieval. This finding is in agreement with the recent study of van Geffen et al. (2021b).

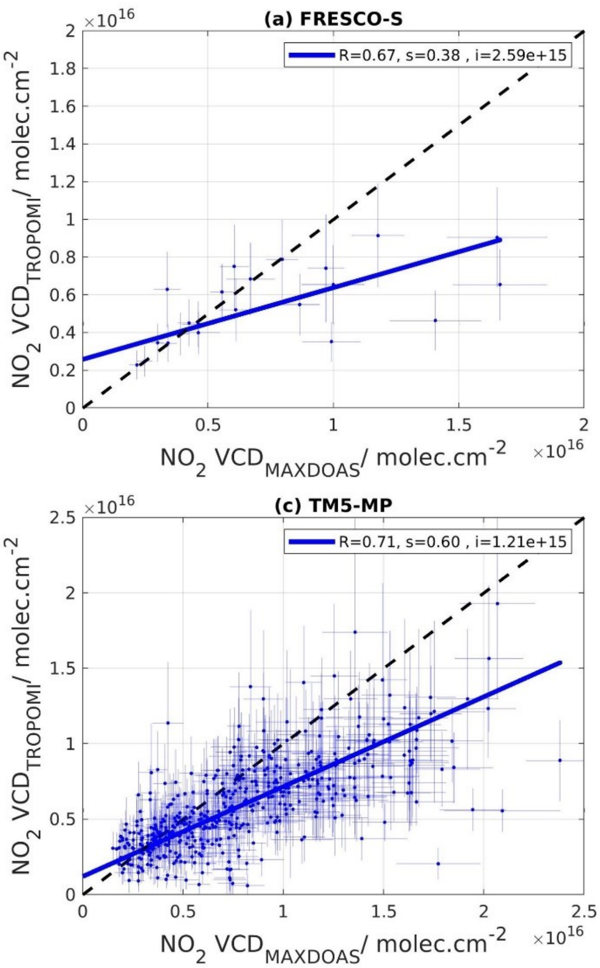

Figure S10. Scatter plots between the tropospheric NO_2 columns derived from the dual-scan MAX-DOAS instrument and the TROPOMI pixels over Brussels. The left plots are for the baseline TROPOMI dataset ((a) and (c) panels), while the right plots correspond to two new versions of TROPOMI datasets ((b): improved FRESCO-S cloud product – DDSv2 product; (d) NO_2 a priori profiles from the CAMS regional CTM ensemble – S5P-CAMS product).

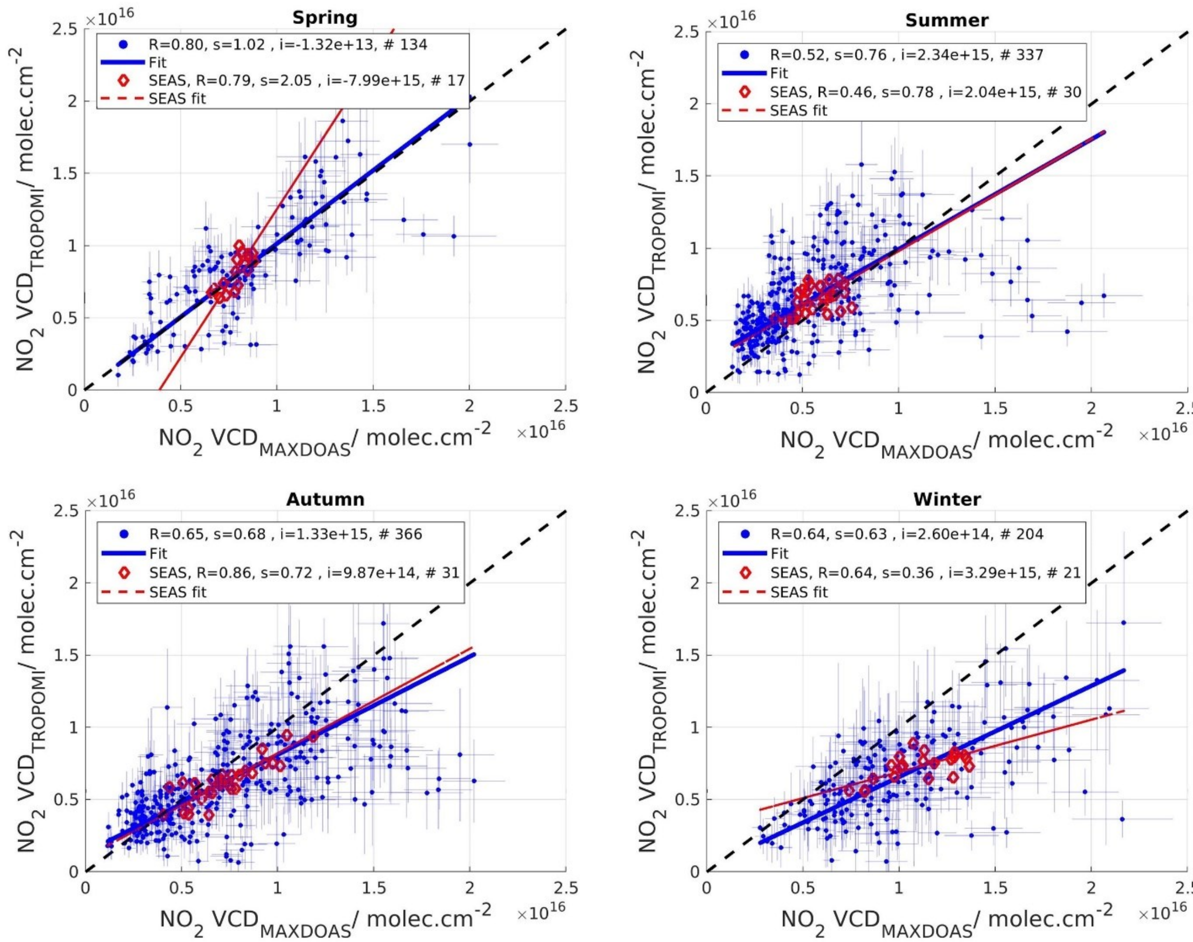

Figure S11. Seasonal scatter plots between the horizontally-averaged MAX-DOAS NO_2 VCDs and TROPOMI NO_2 columns recalculated using median daily MAX-DOAS vertical profiles as a priori information.

References

Chance, K. V. and Spurr, R. J. D.: Ring effect studies: Rayleigh scattering, including molecular parameters for rotational Raman scattering, and the Fraunhofer spectrum, Appl. Optics, 36, 5224– 5230, doi:10.1364/AO.36.005224, 1997.

Fleischmann, O. C., Hartmann, M., Burrows, J. P., and Orphal, J.: New ultraviolet absorption cross-sections of BrO at atmospheric temperatures measured by time-windowing Fourier transform spectroscopy, J. Photoch. Photobio. A, 168, 117–132, 2004.

Meller, R. and Moortgat, G. K.: Temperature dependence of the absorption cross sections of formaldehyde between 223 and 323K in the wavelength range 225–375nm, J. Geophys. Res., 105, 7089–7101, 2000.

Rothman, L.S., Gordon, I.E., Babikov, Y., Barbe, A., Benner, D.C., Bernath, P.F., Birk, M., Bizzocchi, L., Boudon, V., Brown, L.R. and Campargue, A., 2013. The HITRAN2012 molecular spectroscopic database. *Journal of Quantitative Spectroscopy and Radiative Transfer*, *130*, pp.4-50.Seinfeld, J. H. and Pandis, S. N.: Atmospheric Chemistry and Physics: From Air Pollution to Climate Change, John Wiley & Sons, Inc., 1998.

Serdyuchenko, A., Gorshelev, V., Weber, M., Chehade, W., and Burrows, J. P.: High spectral resolution ozone absorption crosssections – Part 2: Temperature dependence, Atmos. Meas. Tech., 7, 625–636, doi:10.5194/amt-7-625-2014, 2014.

Vandaele, A., Hermans, C., Simon, P., Carleer, M., Colin, R., Fally, S., Mérienne, M., Jenouvrier, A., and Coquart, B.: Measurements of the NO2 absorption cross-section from 42000cm−1 to 10000cm−1 (238–1000nm) at 220K and 294K, J. Quant. Spectrosc. Ra., 59, 171–184, 1998.